공학석사 학위논문

The Effect of Geometric conditions on the Instability in Gas Centered Liquid Annular Jet

기체 중심 액체 환상형 제트에서의 기하학적 형상에 따른 불안정 특성 효과

2012년 6월

서울대학교 대학원

기계항공공학부

정 재 묵

The Effect of Geometric conditions on the Instability in Gas Centered Liquid Annular Jet

지도교수 윤 영 빈

이 논문을 공학석사 학위논문으로 제출함
2012 년 6 월

서울대학교 대학원
기계항공공학부
정 재 묵

정재묵의 공학석사 학위논문을 인준함
2012 년 6 월

위 원 장 _____ (인)

부위원장 _____ (인)

위 원 _____ (인)

Abstract

The Effect of Geometric conditions on the Instability in Gas Centered Liquid Annular Jet

Jae Mook Chung

School of Mechanical and Aerospace Engineering

The Graduate School

Seoul National University

The break-up leading to droplets of the liquid spray is used in variety of industrial and applications, but the basic mechanism of the basic mechanism of the break-up is still not completely discovered. Since, the co-flow stream can be used as the oxidizer or fuel and help the atomization of the liquid sheet, the study with co-flow stream has been conducted for many years.

The study of basic mechanism leading to the break-up has been conducted in two types of geometry, the planar and axisymmetric configurations. Since it can neglect the edge effects due to the surface tension and is easy to visualize, the planar type is used widely more than axisymmetric type. The basic mechanism of the liquid sheet perturbation is not that different, when studying the axisymmetric type, the surface tension effect cannot be neglected since the length between the liquid sheets are narrow.

This study addresses the characteristics of the gas centered liquid annular sheet to focus on the instabilities of the spray. It is known that the instability of the spray can cause the liquid flow rate oscillation leading to the combustion instability. To characterize the spray oscillation on the gas

centered liquid annular sheet, two measurements method are conducted. To measure the instability wave length, and distinguish the instability mode of the liquid sheet, Indirect Photography is used. The laser diagnostics is used to measure the frequency of the instability.

The first part of the thesis introduces apparatus and experimental methods.

At the second part of this study, the instability mode is separated which differs with momentum ratio of the spray and the instability characteristics are analyzed. As the gas-liquid momentum ratio increases, the wavelength of the spray oscillation decreased and frequency increased. With the increase of recess ratio which used as the geometric condition, the wavelength increased and frequency decreased.

Consequently, it is appeared that not only gas-liquid momentum ratio but also recess ratio can affect the liquid sheet instability.

Keywords: Gas centered liquid annular injector, Indirect Photography, Recess ratio, Momentum ratio, Spray oscillation

Student Number: 2010-23232

Contents

List of Tables

List of Figures

Nomenclature

Alphabet

c	wave propagation speed
c_i	normalized wave propagation speed
d_g	center orifice exit diameter
d_l	outer orifice exit diameter
f	spray oscillation frequency
k	normalized wavelength constant
h	liquid sheet thickness
MR	momentum ratio
r_g	center orifice exit radius
Re_g	gas Reynolds number
Re_l	liquid Reynolds number
RR	recess ratio
St	Strouhal number
U_l	liquid exit velocity
U_g	gas exit velocity
U_r	gas-liquid relative velocity
x	downstream position from the exit nozzle

Greek

λ	spray oscillation wavelength
σ	liquid surface tension
ρ_g	gas density
ρ_l	liquid density

Chapter 1. INTRODUCTION

1.1 Liquid sheet instability

The break-up leading to droplets of the liquid spray is used in variety of industrial and applications, but the basic mechanism of the basic mechanism of the break-up is still not completely discovered. From numerous studies, it is reported that the instabilities triggered at the near region, lead the sheet breakup. Some studies reported that the existence of the co-flow stream can help the breakup of the liquid sheet. However, these instabilities called as self-pulsation, also lead to the combustion instability. Fig 1.1 Shows the mechanism of the relation of spray oscillation and combustion instability.

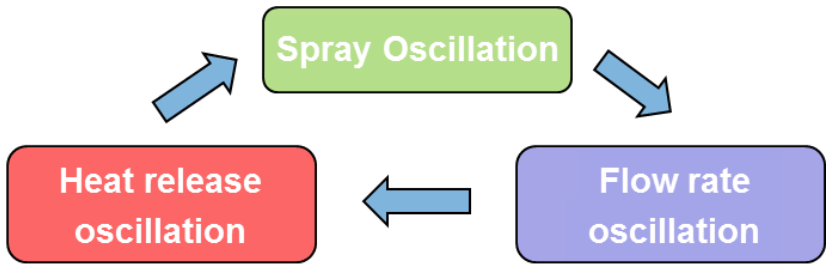

Fig. 1.1 The effect of liquid sheet oscillation

Since, the co-flow stream can be used as the oxidizer or fuel and help the atomization of the liquid sheet, the study with co-flow stream has been conducted for many years.

The study of basic mechanism leading to the break-up has been conducted

in two types of geometry, the planar and axisymmetric configurations. Since it can neglect the edge effects due to the surface tension and is easy to visualize, the planar type is used widely more than axisymmetric type. The basic mechanism of the liquid sheet perturbation is not that different, when studying the axisymmetric type, the surface tension effect cannot be neglected since the length between the liquid sheets are narrow.

1.2 Thin liquid sheet instability

The study of liquid sheet instability has been conducted for many years. Squire et al. investigated the instability of a moving liquid film in an ambient condition, comparing theoretical and experimental values of length of waves, concluding the relationship between the wavelength and liquid velocity.[1] Taylor et al. investigated on capillary waves and found that any disturbance occurs with composed sinusoidal and dilatational waves.[2] Taylor et al. also investigated on disintegration of liquid sheets. In theoretical, the sheet thickness is uniform at the same speed and decreases when it expands, but in experiment, it fluctuated greatly.[3] Dombrowski et al. investigated the drop formation in varying ambient density, concluded that the sheet is disrupted by the aerodynamic waves and the drop size increases with ambient density.[4] Crapper et al. investigated the effect of forced vibration on the thin liquid sheet, comparing with linearized theory which is found that the result of theory disagrees with experimental result.[5]

Experiments for large aspect ratio have been conducted later. Mansour & Chigier investigated on two dimensional air-assisted nozzle, which the liquid sheet is surrounded by two air sheet.[6, 7] It is found that the large droplets were formed from the ligaments and the small droplets were formed from membranes of the spray. The role of the air sheet was come out to help the breakup, disturbing the liquid sheet thickness. The Dynamic behavior of the liquid sheet was also investigated. Along the liquid and gas velocity, the spray frequency changes, which can separated to three regions. The three region, named as zone A, B, and C, differs with the mixture of dilatational and sinusoidal waves. It is concluded that as the gas/liquid velocity ratio increases, the sinusoidal wave seems to be dominant. Lozano et al. investigated the instabilities on the air-assisted injector with spray oscillation frequency, wavelength, propagation speed and SMD along the gas/liquid velocity ratio and liquid sheet thickness.[8-10]

1.3 Liquid sheet instability on annular sheet

The instability and disintegration of the annular liquid is different with typical liquid sheet which has large aspect ratio, since the liquid annular jet converges due to the capillary effects. The study of liquid annular sheet with different geometric configuration has been conducted with the effect of gravity, gas/liquid velocity ratios and inner and outer gas regions. Shen et al. carried out an linear analysis on the annular viscous liquid jet moving in an

inviscid gas medium. The gas medium always enhances the annular jet instability. It is found that the surface tension effect suppresses the instability of the annular viscous liquid jet. The inner gas is revealed to be more effective to breakup up the annular liquid jet than outer gas.[11, 12] Li et al. investigated the spray characteristics parameter such as Sauter mean diameter, mean velocity, velocity fluctuation and droplet number density on the same injector. The result indicated that the droplet axial velocity has a jet-like self-similarity.[13] Ibrahim et al. modeled the nonlinear instability and breakup of an annular liquid sheet in different co-flowing air stream such as, inner, outer and swirling co-flow, since the previous linear theory cannot predict the breakup of the annular sheet. As the co-flow gas stream velocity increases, the liquid sheet breakup hastens, and the inner gas has more effect on the breakup than the outer gas.[14] Wahono et al. conducted a high-speed visualization technique to investigate the primary breakup of an annular liquid sheet. The shear at the interface excites the Kelvin-Helmholtz type instabilities and sinusoidal wave occurs at the gas-liquid interface. Along the downstream, the amplitude of the surface wave grows until it ruptures.[15] Duke et al. used the cross-correlation velocimetry technique on the same injector to investigate the nonlinear instabilities in annular liquid sheets. It is found that two types of physical sources cause the instability of the annular liquid sheets, such as, free shear layer instability and distinct nonlinear rupturing instability.[16, 17]

Although several studies have been conducted to explain the liquid sheet instability in various conditions, the recess ratio effect on the liquid sheet instability has not been reported yet. The recess ratio, which almost used in

swirl injector, it is known that the increase of the recess length develops the liquid droplet size.[18] According to Sankar et al. the recess ratio less than 1.5, the mean size of the liquid droplets increases.[19] Bazarov investigated the high-frequency oscillation and fluctuation which is called self-oscillation or self-pulsation. It is concluded that the recess length is the most important parameter which determines the spray oscillation characteristics.[20] In this study, as a parameter of the instability, wavelength, frequency, propagation speed has been measured using indirect photography and laser diagnostics to examine the effect of the recess ratio on the liquid sheet instability.

Chapter 2. APPARATUS AND EXPERIMENTAL METHOD

2.1 Gas centered liquid annular injector

Designed injectors are shown in fig. 2.1. The outer injector has 8mm diameter with 45mm orifice length and the inner injector has the 5.1mm inner diameter with 6.3mm outer diameter. As the recess ratio increases 0 to 1.5, the depth of the inner injector increases 0 to 7.65 mm.

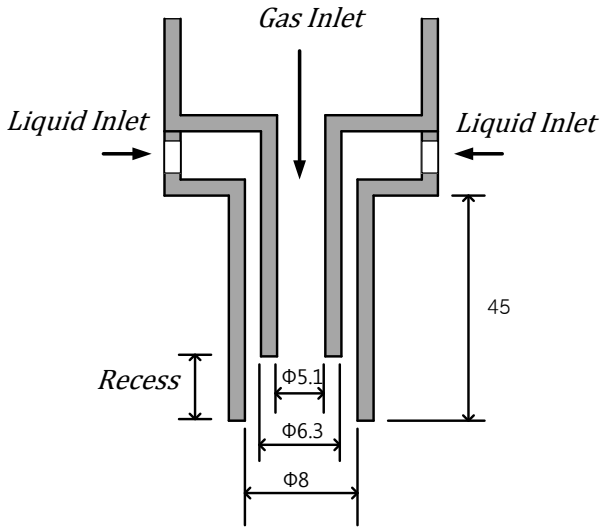

Fig 2.1 Gas centered Liquid annular injector

2.2 Experimental apparatus

The experiment setup is shown in fig. 2.2. The gas centered liquid annular injector was installed at the experimental rig which the gas line was connected at the top of the injector and the liquid line at the side. Air and water were used as gas and liquid. The air flow rate was measured by a mass flow meter (Alicat Scientific ; M-1500SLPM-D), and manually controlled with a gas regulator. The water flow rate was controlled by measuring the pressure before the injector exit with pressure sensor (Sensys ; PTAF0010KAA). The flow rate along the pressure drop before the injector exit is shown in fig 2.3. The experimental rig is sealed with transparent polycarbonate covers with the ceiling open.

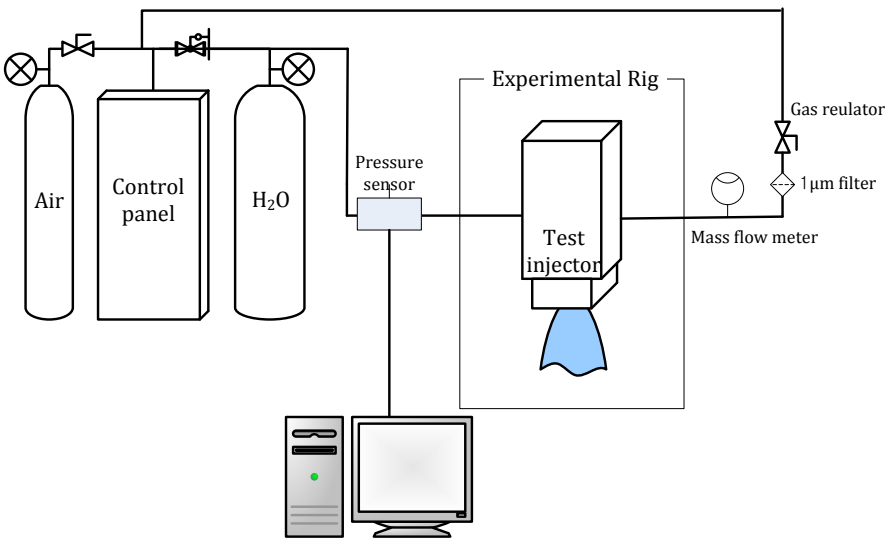

Fig 2.2 Experimental Apparatus

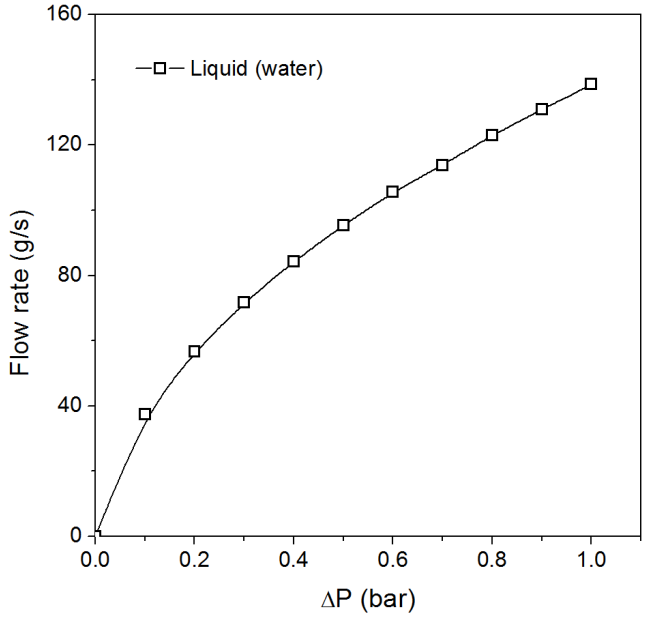

Fig 2.3 Mass flow rate of water along the pressure drop

2.3 Indirect Photography

To define the instability modes and measure the wavelength of the flow oscillation, indirect photography was used. Indirect photography has no difficult to setup but can measure the spray structure efficiently. Fig 2.4 shows the schematic of the indirect photography. A digital camera (Canon EOS 7D, Canon EF 24-70mm f/2.8 L USM) is set at the front and digital strobe (SUGAWARA; S-124M) is set at the back of the spray. The camera and strobe were synchronized with 1/10s. Fig 2.5 shows the typical image of

the spray oscillation.

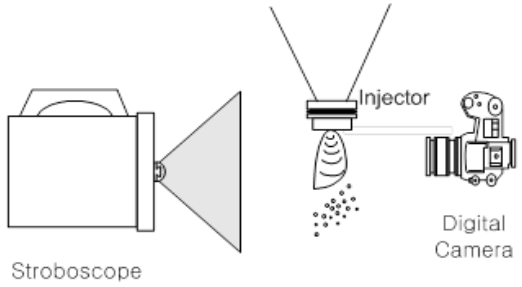

Fig 2.4 Indirect Photography

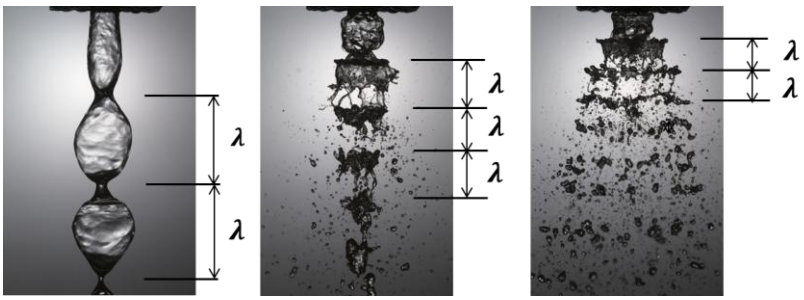

Fig 2.5 Image of the spray oscillation

As the spray oscillation occurs the boundary of the oscillation can be distinguished due to the density difference of the liquid sheet. The first image of the fig 2.5, as the bubble grows up, the liquid sheet thickness becomes thinner while the thickness of the neck becomes thicker since the liquid sheet collapse. At second and the third image of the fig 2.5, the bubble breaks up separating the liquid drop. Due to these separations, the boundary of the oscillation becomes darker. In this study, these darken boundaries were defined as the boundary of the oscillation and measured as wavelength. Each image was converged monochrome photograph and averaged the

brightness of 200 x 80 pixels along the centerline to determine the boundary and avoid the error due to the small droplets. At each image, 2 to 3 wavelengths were measured and to lower the error, the wavelengths of 20 images at each experimental condition were measured.

2.4 Frequency measuring method

Laser diagnostic were used to measure the frequency of the spray oscillation. Fig 2.6 shows the schematic of the laser diagnostic used in this study. Continuous laser, made by He-Ne Laser (GLG 5350), passes the spray applying to the photo detector (DET36 A/M) which is positioned at the back of the spray. Due to the difference of the density along the centerline, the received signal can be transferred by Fast Fourier Transform (FFT) process, which appears to be frequency of the spray oscillation. The sampling rate and sampling number are chosen as 5000, and fig 2.7 shows the result of the FFT process.

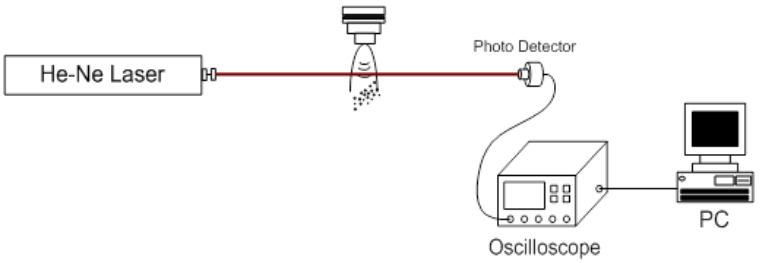

Fig 2.6 Frequency measuring with He-Ne Laser

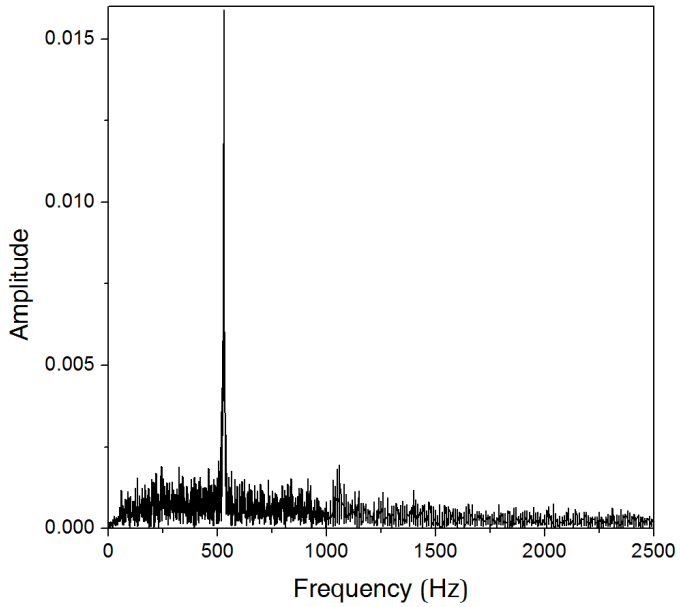

Fig 2.7 Result of FFT process

Since the place where the instability starts to occur differs along the instability mode, such as, at Rayleigh mode, frequency should be measured at the far region from the nozzle exit while it should be measured at near region at Pure puslation mode. Due to this difference, frequency measuring location should be different with instability mode. Fig 2.8 shows the measured location of spray oscillation. The frequency is measured at x/ d_g = 5, 10, 15, Where x is the downstream length from the nozzle exit and d_g is the center nozzle diameter. Fig 2.9 shows the result of the measured frequency with different gas Reynolds number in constant liquid Reynolds number. The result shows that the frequency is independent along the downstream position. This trend was also shown in Mansour & Chigier [7] and Lozano et al.[8].

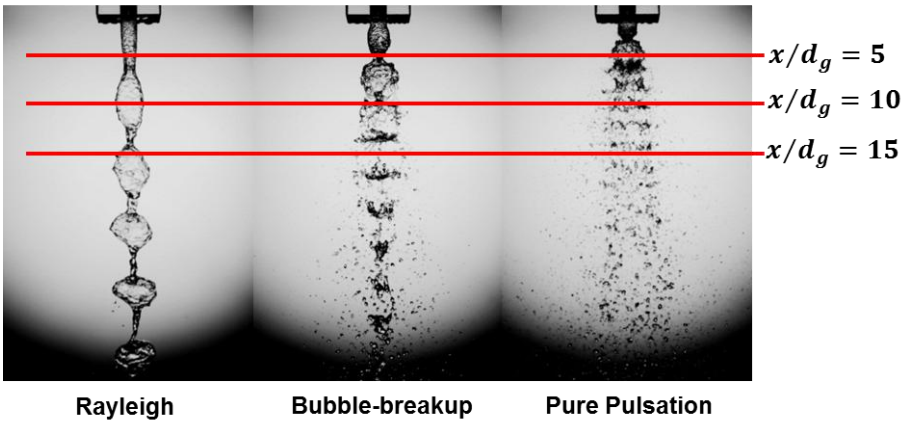

Fig 2.8 Measured location of the spray oscillation

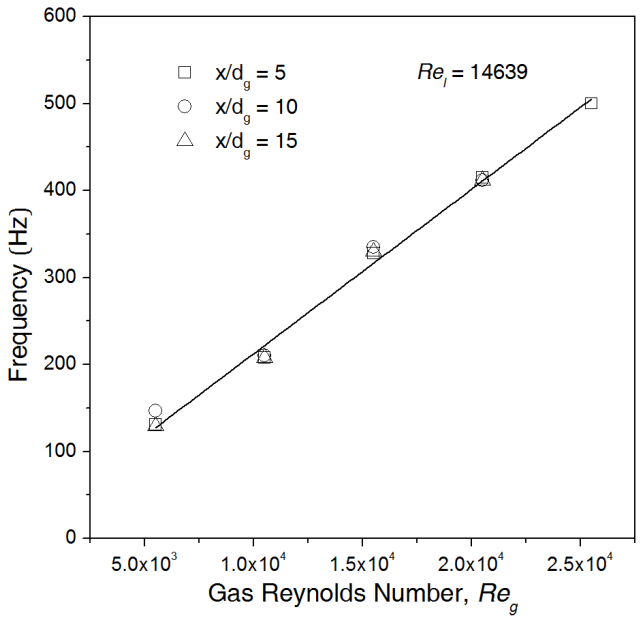

Fig 2.9 Measured frequency along the x/d_g

(Re_l = 14639, U_l = 2.98 m/s)

2.5 Experimental Conditions

Experiments have been performed in an attempt to understand the mechanism of the liquid sheet instability and table 2.1 shows overall experimental conditions. Air flow rates are adopted 5 cases as shown in table 2.1. Water flow rates are also adopted 5 cases. Recess ratio changes 0 to 1.5 with unit 0.5.

Table 2.1 Experimental Conditions

Phase	Liquid	Gas
Fluid	Water	Air
Velocity (m/s)	1.96 ~ 5	15.74 ~ 72.98
Mass flow rate (g/s)	24.92 ~ 95.44	0.39 ~ 2.15
Reynolds number	9680 ~ 24646	5500 ~ 25500
Momentum ratio	0.01 ~ 1.76	
Recess ratio	0, 0.5, 1.0, 1.5	
Outer injector diameter (mm)	8	
Center injector inner diameter (mm)	5.1	
Center injector outer diameter (mm)	6.3	

Chapter 3. RESULT AND DISCUSSION

3.1 Mode transition of instability

Fig 3.1 and 3.2 shows the mode transition and mechanism of the spray oscillation at the current experimental conditions. Choi et al.[21] defined the mode transition of the gas centered annular liquid spray along the liquid Reynolds number and Weber number such as Rayleigh, Bubble breakup, Pure pulsation. From the images, fig 3.1-(a) shows that without center air flow, the water sheet collapse at the near region after the nozzle exit due to the surface tension effect. When the center air starts to flow, the collapsed liquid sheet separates, flowing parallel to the air flow. As the air flow velocity increases, the gap of the annular decreases since the pressure of the inside of the annular liquid sheet starts to become lower. Due to the surface tension, the decreased gap of the liquid sheet creates a neck. The air flow cannot flow through the neck, expanding the liquid sheet to radial direction. After the next neck creation, the bubble formed and this process repeats. (Rayleigh mode, Fig 3.1-(b)) Kendall [22] reported that the diameter of the bubble grows up until twice of the diameter of the nozzle exit. As the air flow velocity increases, the bubble sheet cannot withstand the radial direction pressure, leading to the bubble breakup. However the droplet of the liquid do not ends up to atomization due to the insufficient velocity profile of the radial direction of the air flow, collapsing due to the surface tension of the water. (Bubble breakup mode, Fig 3.1-(c)) As the air flow velocity is enough to atomize the

droplet, the spray starts to have positive spray angle, atomizing along the downstream. (Pure pulsation, Fig 3.1-(d))

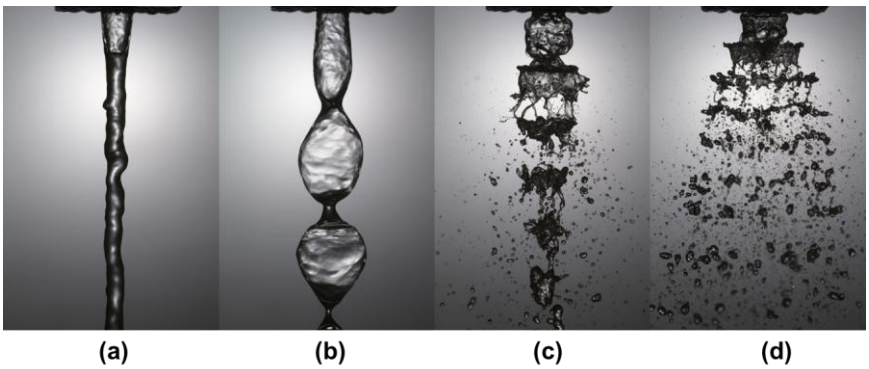

Fig 3.1 Mode transition of spray oscillation –

(a) No air, (b) Rayleigh, (c) Bubble breakup, (d) Pure pulsation

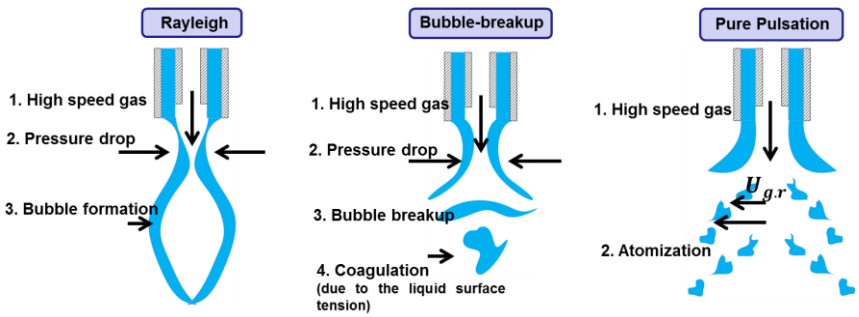

Fig 3.2 Instability mechanism

Fig 3.3 shows the boundary of the instability mode along the gas and liquid Reynolds number. As the gas Reynolds number increases, the instability mode changes Rayleigh, Bubble-breakup and Pure pulsation. The opposite process occurs when the liquid Reynolds number increases. As the recess ratio

increases, the boundary of the instability modes move back along the gas Reynolds number at the same experimental conditions. It seems that the recess affects the gas and liquid flows to exchange those momentums each other, decreasing the gas velocity and increasing the liquid velocity.

Liquid Reynolds number	Gas Reynolds number				
14639	5500	10500	15500	20500	25500
RR = 0.0					
RR = 0.5					
RR = 1.0					
RR = 1.5					

(a)

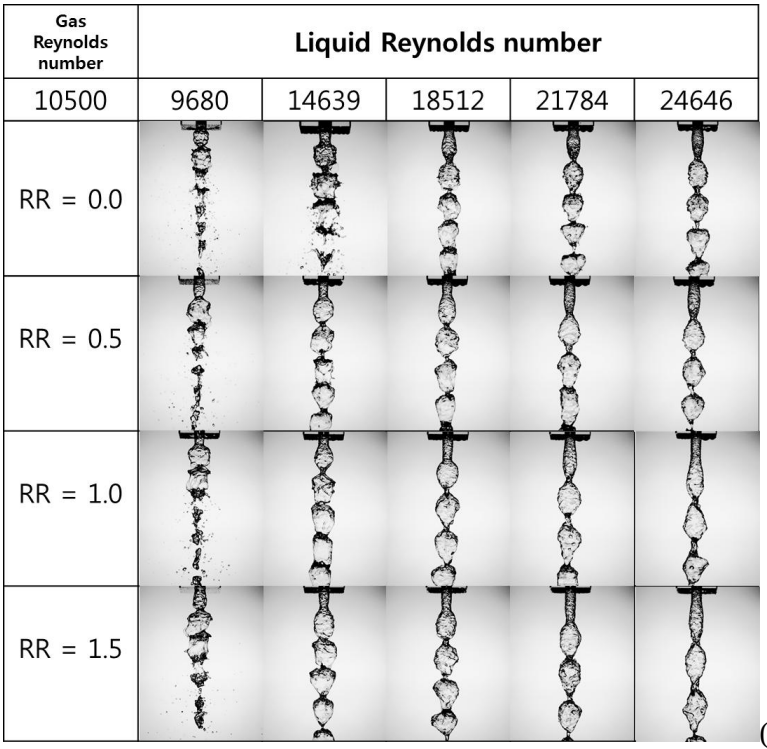

(b)

Fig 3.3 Mode transition boundary

(a) Re_l = 14639, U_l = 2.98 m/s, (b) Re_g = 10500, U_g = 30 m/s

3.2 Effect on wave length

Fig 3.4 shows the measured wave length of this study. In fig 3.4-(a), the square with solid line denotes the liquid Reynolds number 9680, the circle with dash line denotes 14639, the triangle with dot line denotes 18512, the inverted triangle with dash-dot line denotes 21784 and the diamond with dash-dash-dot denotes 24646. In the same condition of same liquid Reynolds number, wavelength of the spray oscillation decreases with the increase of gas Reynolds number. In fig 3.4-(b), the square with solid line denotes the gas Reynolds number 5500, the circle with dash line denotes 10500, the triangle with dot line denotes 15500, the inverted triangle with dash-dot line denotes 20500 and the diamond with dash-dash-dot line denotes 25500. In the same condition of same gas Reynolds number, wavelength of the spray oscillation increases with the increase of liquid Reynolds number. According to Park et al. [23], the linear inviscid theory predicts the fastest growing wavelength λ as

$$\lambda = \frac{4\pi\sigma}{\rho_g U_r}$$

Where σ is the surface tension of the liquid sheet, ρ_g is the density of the interacting ambient air, U_r is the relative velocity between gas and liquid which can be denoted as (U_g-U_l). In this study, the gas velocity is higher than the liquid velocity resulting that the increase of U_g for a constant U_l may decrease the wavelength of the spray oscillation and the increase of U_l for a constant U_g may increase the wavelength.

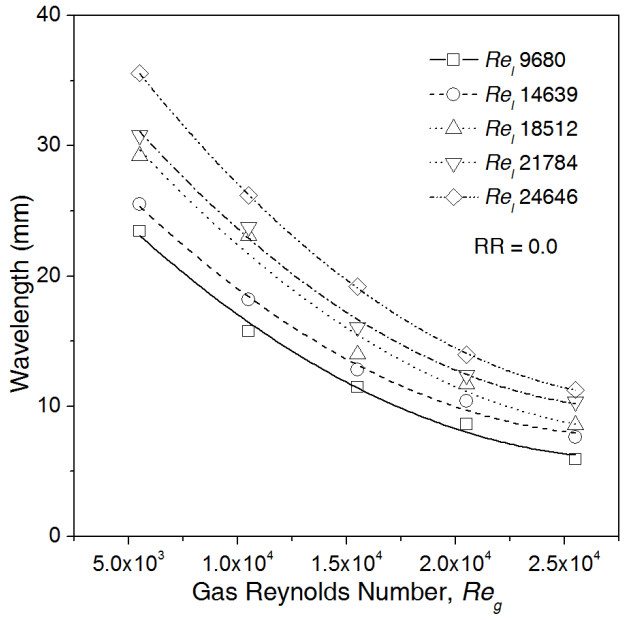

(a)

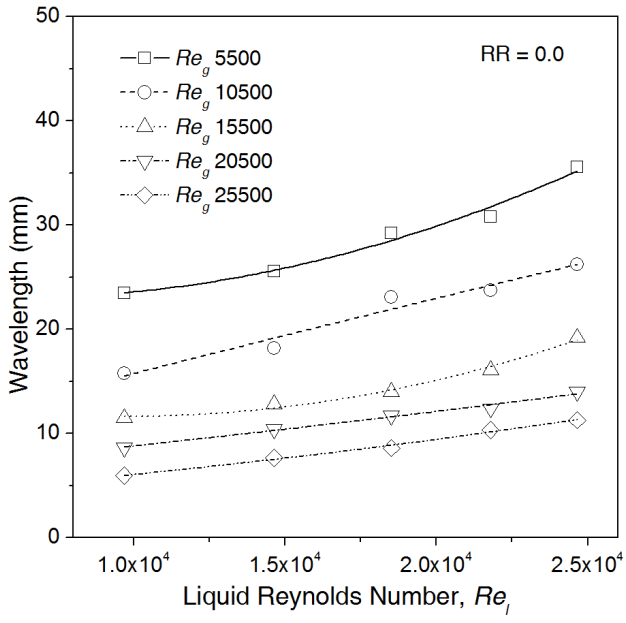

(b)

Fig 3.4 Effect on Wavelength along the

(a) gas Reynolds number, (b) liquid Reynolds number

The effect of recess ratio is shown in fig 3.5. The square with solid line denotes the recess ratio 0.0, the circle with dash line denotes 0.5, the triangle with dot line denotes 1.0 and the inverted triangle with dash-dot line denotes 1.5. As mentioned at Chapter 3.1, the boundaries of the instability transition move back while the recess ratio increases due to the momentum exchange between the gas and liquid, changing the exit velocity which the gas velocity decreases and liquid increases. This leads to the decrease of the relative velocity, U_r, increasing the λ. The increase of recess ratio means that the length to exchange the momentum between gas and liquid, so it can be predicted that the relative velocity, U_r may decrease, increasing the λ. However, from fig. 3.5, it is appeared that until recess ratio 1.0 follows this trend, but at the recess ratio 1.5, the wavelength seems to be lower than 1.0.

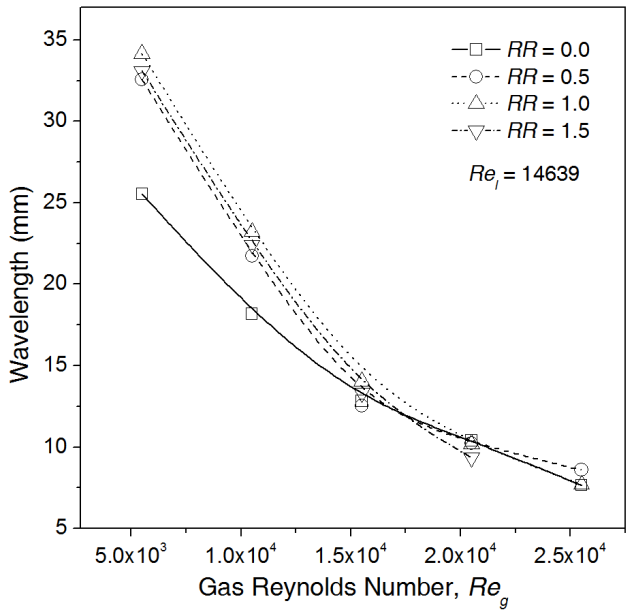

(a)

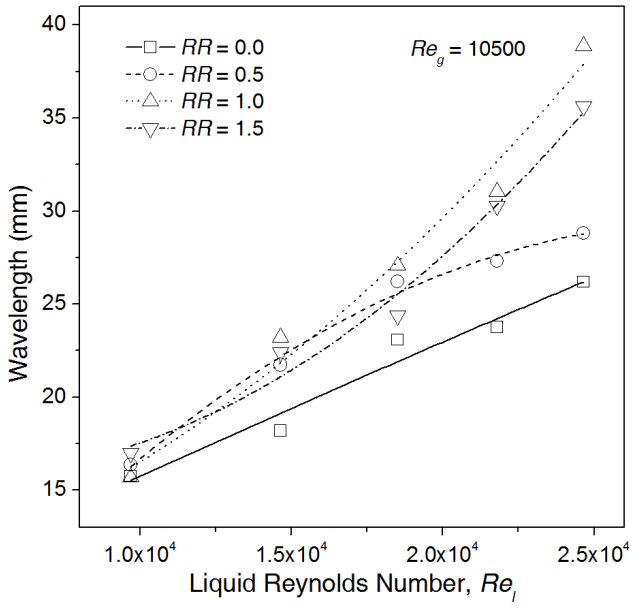

(b)

Fig 3.5 Effect on Wavelength comparing with recess ratio

(a) Re_l = 14639, U_l = 2.98 m/s, (b) Re_g = 10500, U_g = 30 m/s

Fig 3.6 shows the linear dependence between half wavelength and U_l/U_g ratio. According to Lozano et al.[10], this relationship can be fitted as

$$\frac{\lambda}{2} = kh\frac{U_l}{U_g}$$

From the result of Lozano's, the *k* remained constant and equal to 300, while the liquid sheet thickness changed. In this study, the value of *k* showed 81.36. The reason of the difference between Lozano's result and this experiment is considered to be the geometrical difference of the liquid sheet. Lozano performed the experiment in the planar sheet, which the wavelength can grow up continuously in its growth rate, however in this study, the annular liquid sheet was used, the wavelength cannot grow up since the radius of the annular is not enough large leading the oscillation coagulate and starts the 0° phase.

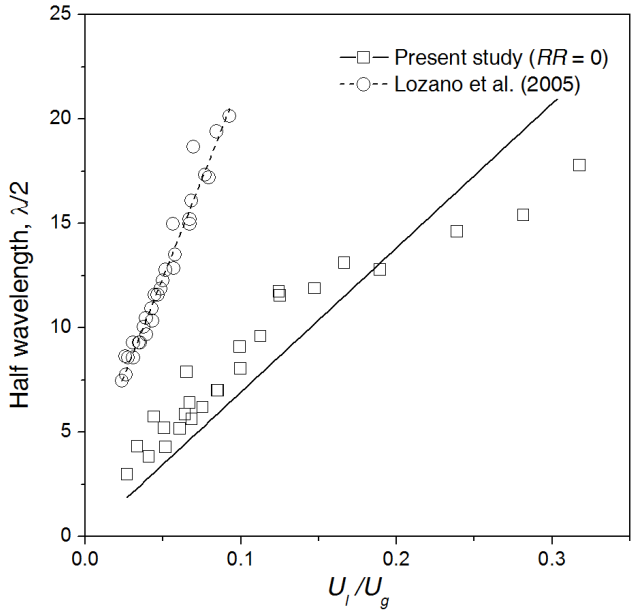

Fig 3.6 Linear dependence between half wavelength and U_l/U_g comparing with the result of Lozano et al (2005)

Fig 3.7 shows the relationship between half wave length and U_l/U_g ratio with recess ratio. At the same U_l/U_g ratio, the half wavelength increased with recess ratio. The value of k with each recess ratio appeared to be 81.35, 107.24, 119.13 and 113.82

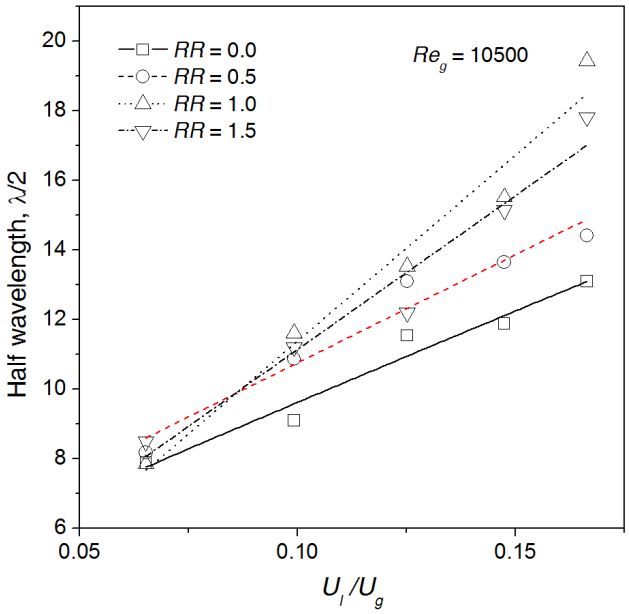

Fig 3.7 Linear dependence between half wavelength and U_l/U_g comparing with different recess ratio

Lozano et al.[10] also showed another relationship. The wavelength, divided by square root of the sheet thickness and Momentum ratio ($\frac{\rho_g U_g^2 d_g}{\rho_l U_l^2 d_l}$) are used as non-dimensional group. This relationship can be fitted as

$$\frac{\lambda}{\sqrt{\mathrm{hr_g}}} = \frac{k}{\sqrt{MR}}$$

From the result of Lozano, the *k* is constant, which the value is 20.39. Also in this study, k seems to be constant, the value is 5.4. The reason of different value which Lozano reported and in this study can be explained as same as the result of half wavelength and U_l/U_g ratio. Fig 3.8 and 3.9 shows the plot of

non-dimensional wavelength and momentum ratio, comparing with Lozano's result and different recess ratio.

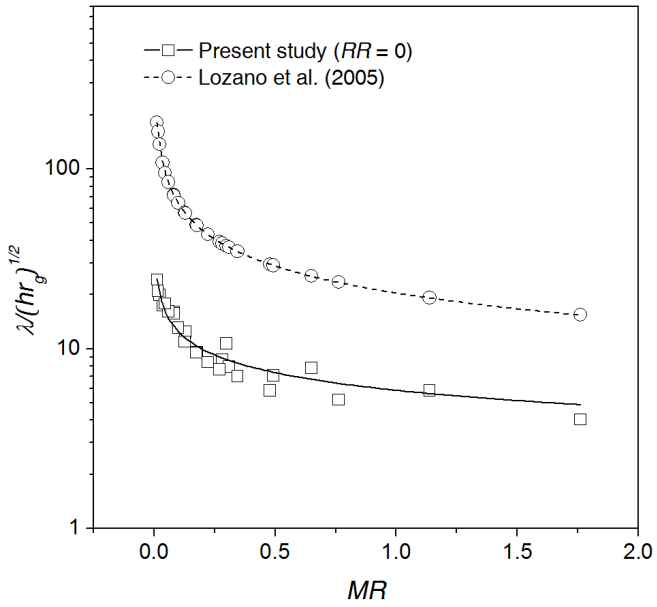

Fig 3.8 Non-dimensional wavelength as a function of Momentum ratio, comparing with the result of Lozano et al (2005)

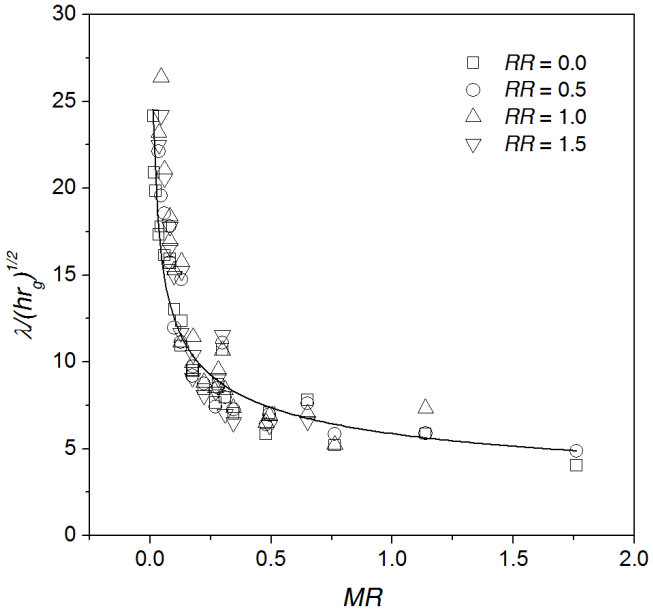

Fig 3.9 Non-dimensional wavelength as a function of Momentum ratio, comparing with recess ratio

3.3 Effect on frequency

Fig 3.10 shows the measured frequency of this study. In Fig 3.10-(a), the square with solid line denotes the liquid Reynolds number 9680, the circle with dash line denotes 14639, the triangle with dot line denotes 18512, the inverted triangle with dash-dot line denotes 21784 and the diamond with dash-dash-dot denotes 24646. In the same condition of same liquid Reynolds number, frequency of the spray oscillation increases with the increase of gas Reynolds number. In fig 3.10-(b), the square with solid line denotes the gas Reynolds number 5500, the circle with dash line denotes 10500, the triangle with dot line denotes 15500, the inverted triangle with dash-dot line denotes 20500 and the diamond with dash-dash-dot line denotes 25500. In the same condition of same gas Reynolds number, frequency of the spray oscillation slightly increased with the increase of liquid Reynolds number. According to Lozano et al.[9], the frequency curves as a function of water velocity have a maximum value, which its region named as zone B by Mansour & Chigier [7]. In this study, the growth of frequency along the liquid Reynolds number seems to be similar which Lozano presented. This regime is defined where the breakup mode exhibits streamwise ligaments. From Lozano, the best atomization characteristics occur in this zone, with a dominant sinusoidal oscillation of the liquid sheet, rapid amplitude growth, large spray angle and small droplet sizes.

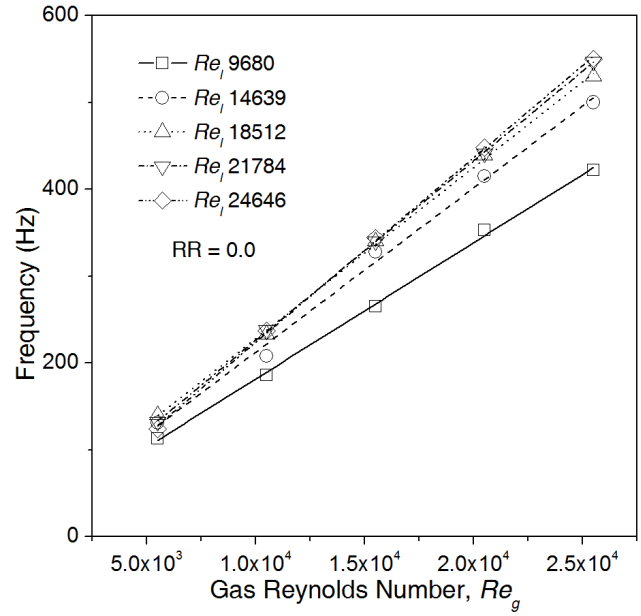

(a)

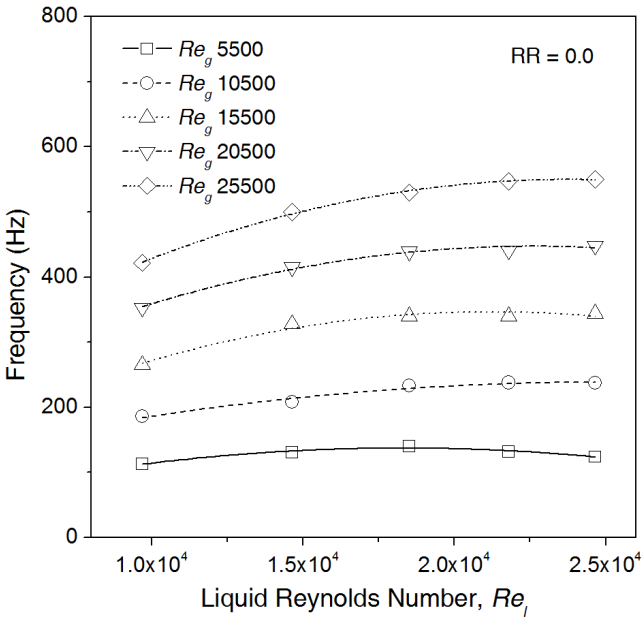

(b)

Fig 3.10 Effect on frequency along the

(a) gas Reynolds number, (b) liquid Reynolds number

The effect of recess ratio is shown in Fig 3.11. The square with solid line denotes the recess ratio 0.0, the circle with dash line denotes 0.5, the triangle with dot line denotes 1.0 and the inverted triangle with dash dot line denotes 1.5. It is appeared that frequency decreases with recess ratio. If there is a momentum exchange between gas and liquid inside of the recess, the frequency should decrease with gas Reynolds number and increased with gas Reynolds number as the recess ratio increased, since frequency increased with of gas and liquid Reynolds number. However, from fig 3.11, the trend seems to be opposite. It is considered that the decreased gas velocity is larger than the increased liquid velocity, since the density of the liquid is 1000 times larger than the gas density. This can be explained by fig 3.10, which the change rate of the frequency is larger at the independence of gas Reynolds number than the liquid Reynolds number. However, recess ratio 1.5 do not follow the trend as it is seemed at the result of wavelength.

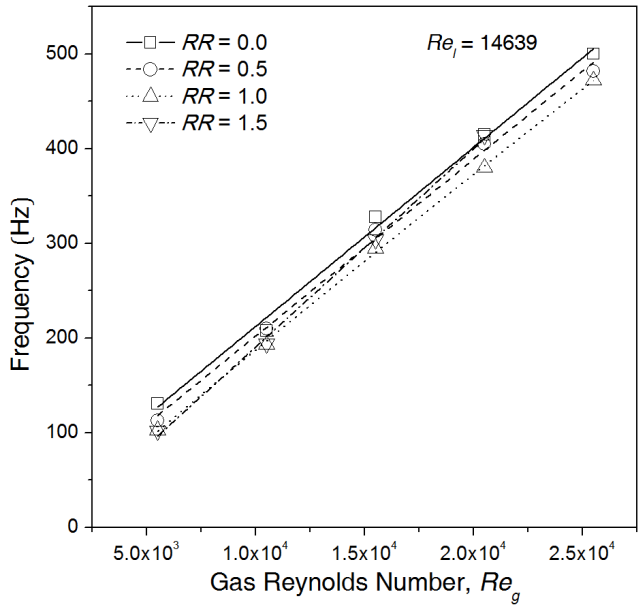

(a)

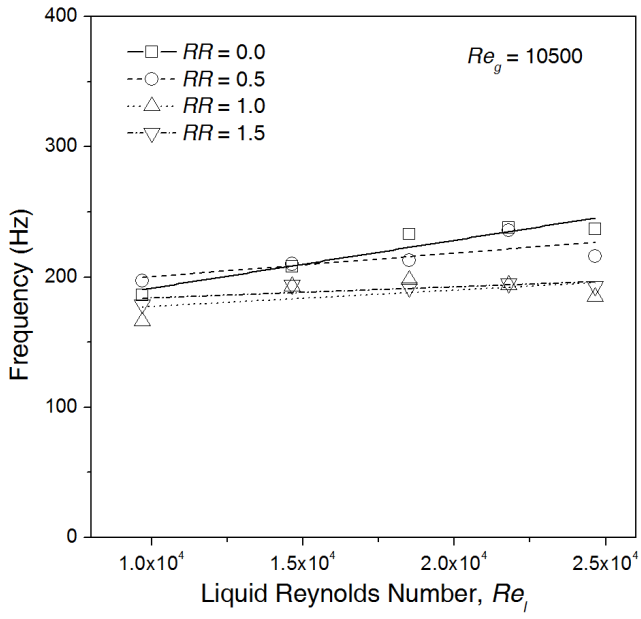

(b)

Fig 3.11 Effect on Frequency comparing with recess ratio

(a) Re_l = 14639, U_l = 2.98 m/s, (b) Re_g = 10500, U_g = 30 m/s

From the measured frequency, Strouhal number can be obtained by multiplying geometric average of liquid sheet thickness and center gas radius and dividing gas velocity. It can be presented as

$$St = \frac{f\sqrt{hr_g}}{U_g}$$

Fig. 3.12 shows the Strouhal number which obtained from this study and the result of Lozano et al.[10] with momentum ratio. The order of the Strouhal number obtained is in the range of 0.01 to 0.15 and this is the typical value of the liquid sheet instability. The result of Lozano also shows in the similar range. Fig 3.13 shows the Strouhal number along the momentum ratio comparing with recess ratio. As the frequency decreased with recess ratio, Strouhal number also shows the same trend, but all of the results are in the same range as recess 0.0 does.

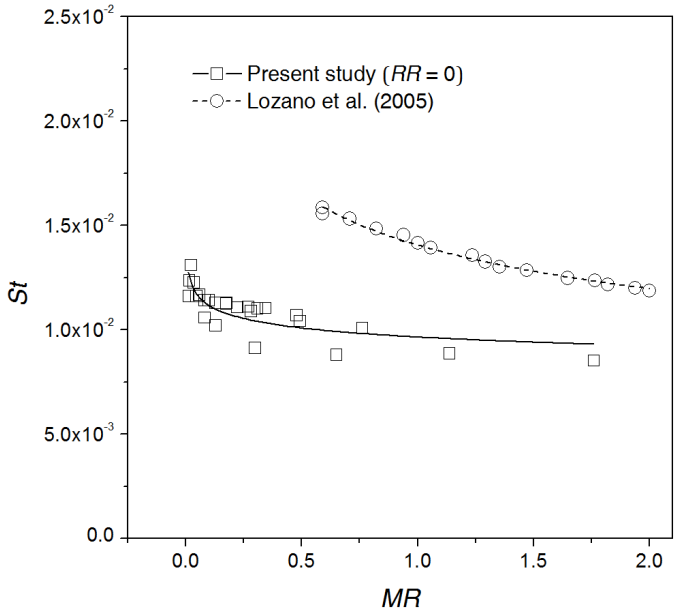

Fig 3.12 Strouhal number along the momentum ratio (RR = 0)

comparing with result of Lozano et al (2005)

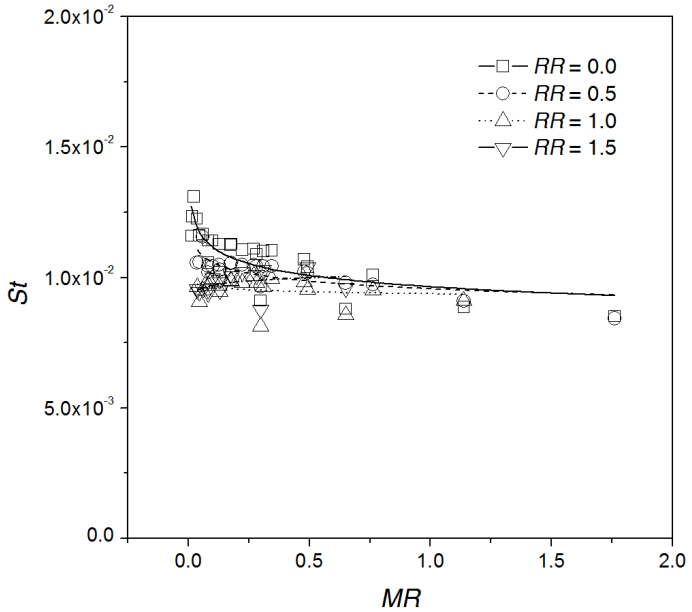

Fig 3.13 Strouhal number comparing with recess ratio

3.4 Effect on wave propagation speed

Since, measuring the wave propagation speed is difficult due to its variation along the downstream position, it is calculated as

$$c = f\lambda$$

where *c* is the wave propagation speed. Fig 3.14 shows the calculated wave propagation speed of this study. In fig 3.14-(a) the square with solid line denotes the liquid Reynolds number 9680, the circle with dash line denotes 14639, the triangle with dot line denotes 18512, the inverted triangle with dash dot line denotes 21784 and the diamond with dash dash-dot denotes 24646. In the same condition of same liquid Reynolds number, wave propagation speed of the spray oscillation slightly increased with the increase of gas Reynolds number is not that significant. In fig 3.14-(b), the square with solid line denotes the gas Reynolds number 5500, the circle with dash line denotes 10500, the triangle with dot line denotes 15500, the inverted triangle with dash-dot line denotes 20500 and the diamond with dash-dash-dot line denotes 25500. In the same condition of same gas Reynolds number, wave propagation speed of the spray oscillation seems to increase with the increase of liquid Reynolds number. According to Lozano et al.[9], it is customary to assume that the propagation speed is identical to the liquid velocity. However, Lozano calculated the propagation speed using the same method in which this study used and concluded that the propagation speed exceeds the liquid velocity due to the gas acceleration to the liquid. Fig 3.15 shows the normalized wave propagation speed ($c_i = c/U_l$) along the gas and liquid

Reynolds number with different conditions. From fig 3.15-(a), as the gas Reynolds number increases, the propagation speed slightly increases which all of the propagation speed of gas Reynolds number coming together of value 1.2. From fig 3.15-(b), as the liquid Reynolds number increases, the value of c_i approaches to 1. From this trend it can be considered that for high gas/liquid velocity ratios, gas accelerates the liquid sheet, and the for the low gas/liquid velocity ratios, liquid sheet tolerate the acceleration of the gas due to its momentum, corresponding the propagation speed identically to its velocity.

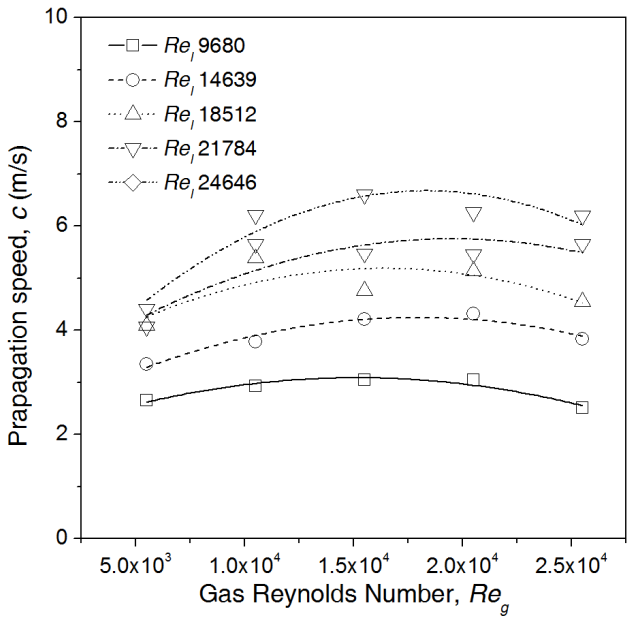

(a)

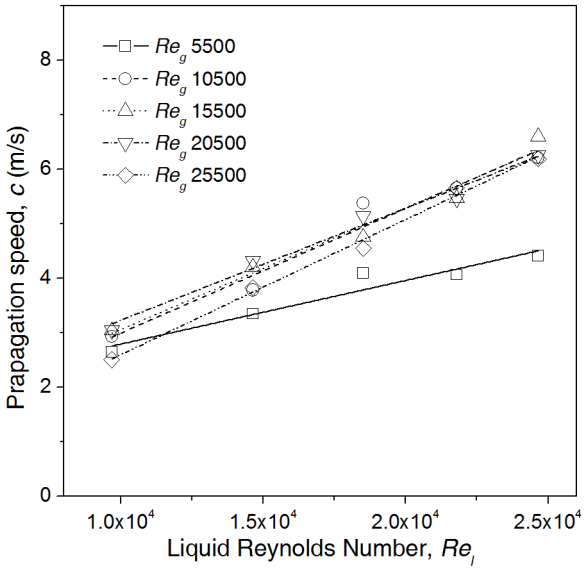

(b)

Fig 3.14 Effect on propagation speeed along

(a) the gas Reynolds number (b) the liquid Reynolds number

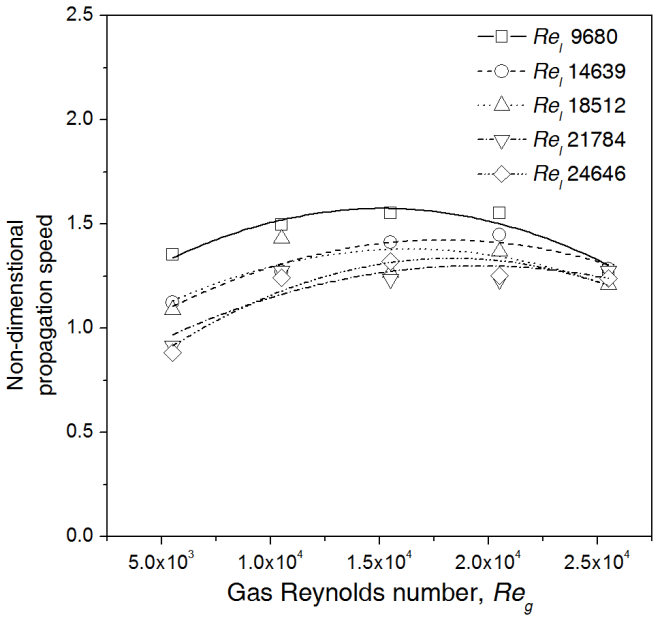

(a)

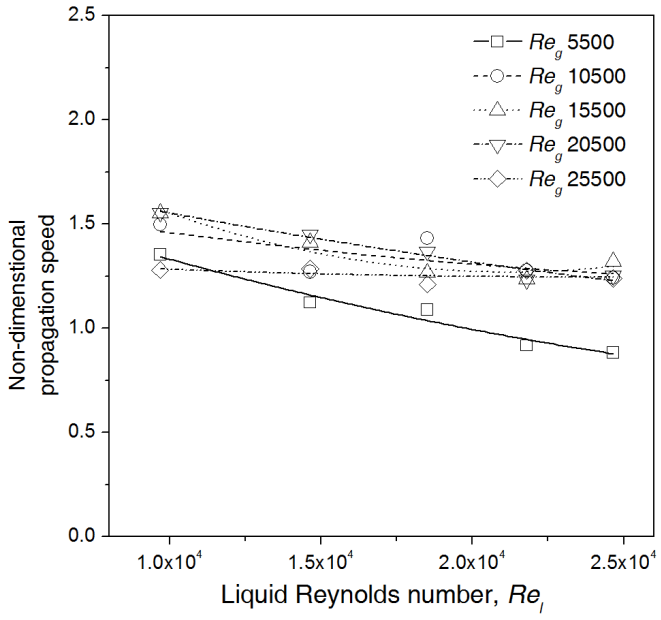

(b)

Fig 3.15 Non-dimensional propagatio speed along the

(a) the gas Reynolds number (b) the liquid Reynolds number

Fig 3.16 shows the effect of recess ratio on propagation speed. All of the recess ratios show the same trend on the propagation speed with gas and liquid Reynolds number as the recess ratio 0.0 showed, but the trend along the recess ratio, shown at wavelength and frequency seems to be absent.

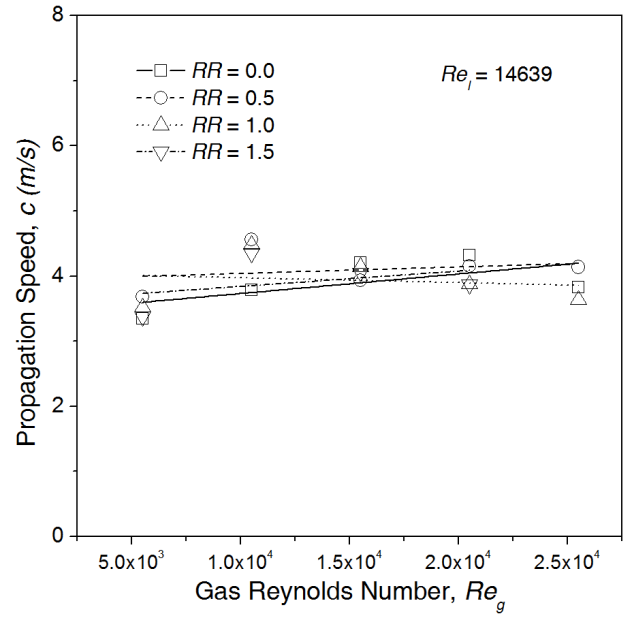

(a)

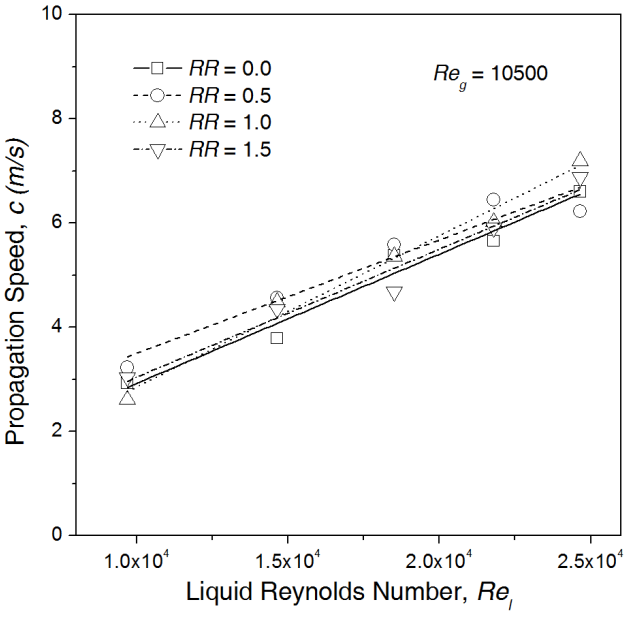

(b)

Fig 3.16 Effect on propagation speed comparing with recess ratio

(a) Re_l = 14639, U_l = 2.98 m/s (b) Re_g = 10500, U_g = 30 m/s

Chapter 4. CONCLUSION

An experiment of gas centered liquid annular spray was conducted with geometric variation. In a condition of gas centered liquid annular injector which the instability can be seen, the effect of liquid, gas Reynolds number and recess ratio on the spray oscillation wavelength, frequency, propagation speed are investigated by indirect photography and laser diagnostics measurements. Furthermore, the normalized wavelength, Strouhal number and normalized propagation speed which previous studies investigated are also examined.

1. Wavelength of the spray oscillation decreases with gas Reynolds number and increases with liquid Reynolds number.
2. Gas Reynolds number has more effect on increasing on frequency of the spray oscillation than liquid Reynolds number.
3. Wave propagation speed increases both with gas Reynolds number and liquid Reynolds number, but liquid Reynolds number appeared to have more effect.
4. As recess ratio increases, wavelength increased while frequency decreased.
5. The recess ratio appeared to have no significant effect on wave propagation speed.

Bibliography

1. Squire, H.B., *Investigation of the instability of a moving liquid film.* British Journal of Applied Physics, 1953. **4**(6): p. 167.
2. Taylor, G., *The Dynamics of Thin Sheets of Fluid. II. Waves on Fluid Sheets.* Proceedings of the Royal Society of London. Series A. Mathematical and Physical Sciences, 1959. **253**(1274): p. 296-312.
3. Taylor, G., *The Dynamics of Thin Sheets of Fluid. III. Disintegration of Fluid Sheets.* Proceedings of the Royal Society of London. Series A. Mathematical and Physical Sciences, 1959. **253**(1274): p. 313-321.
4. Dombrowski, N. and P.C. Hooper, *The effect of ambient density on drop formation in sprays.* Chemical Engineering Science, 1962. **17**(4): p. 291-305.
5. Crapper, G.D., N. Dombrowski, and G.A.D. Pyott, *Large Amplitude Kelvin-Helmholtz Waves on Thin Liquid Sheets.* Proceedings of the Royal Society of London. A. Mathematical and Physical Sciences, 1975. **342**(1629): p. 209-224.
6. Mansour, A. and N. Chigier, *Disintegration of liquid sheets.* Physics of Fluids A: Fluid Dynamics, 1990. **2**(5): p. 706-719.
7. Mansour, A. and N. Chigier, *Dynamic behavior of liquid sheets.* Physics of Fluids A: Fluid Dynamics, 1991. **3**(12): p. 2971-2980.
8. Lozano, A., et al., *Experimental and numerical study of the atomization of a planar liquid sheet.* Atomization and Sprays, 1996.

6(1): p. 77-94.

9. Lozano, A., et al., *Longitudinal instabilities in an air-blasted liquid sheet.* Journal of Fluid Mechanics, 2001. **437**: p. 143-173.
10. Lozano, A., et al., *The effects of sheet thickness on the oscillation of an air-blasted liquid sheet.* Experiments in Fluids, 2005. **39**(1): p. 127-139.
11. Shen, J. and X. Li, *Instability of an annular viscous liquid jet.* Acta Mechanica, 1996. **114**(1): p. 167-183.
12. Shen, J. and X. Li, *Breakup of annular viscous liquid jets in two gas streams.* Journal of Propulsion and Power, 1996. **12**(4): p. 752-759.
13. Li, X. and J. Shen, *Experimental study of sprays from annular liquid jet breakup.* Journal of Propulsion and Power, 1999. **15**(1): p. 103-110.
14. Ibrahim, A.A. and M.A. Jog, *Nonlinear instability of an annular liquid sheet exposed to gas flow.* International Journal of Multiphase Flow, 2008. **34**(7): p. 647-664.
15. Wahono, S., et al., *High-speed visualisation of primary break-up of an annular liquid sheet.* Experiments in Fluids, 2008. **44**(3): p. 451-459.
16. Duke, D., D. Honnery, and J. Soria, *A cross-correlation velocimetry technique for breakup of an annular liquid sheet.* Experiments in Fluids, 2010. **49**(2): p. 435-445.
17. Duke, D., D. Honnery, and J. Soria, *Experimental investigation of nonlinear instabilities in annular liquid sheets.* Journal of Fluid

Mechanics, 2012. **691**: p. 594-604.

18. Sasaki, M., Sakamoto, H., Takahashi, M., Tomita, T., & Tamura, H, *Comparative Study of Recessed and Non-recessed Swirl Coaxial Injectors.* 33rd AIAAASMESAEASEE Joint Propulsion Conference, 1997.

19. Sankar. S. V., W.G., Brena de La Rosa. A., Rudoff. R. C., Isakovic. A., Bachalo. W. D., *Characterization of coaxial rocket injector sprays under high pressure environments.* AIAA, Aerospace Sciences Meeting and Exhibit, 30th, Reno, NV, 1992.

20. Bazarov, V.G., *Self-pulsation in coaxial injectors with central swirl liquid stage.* AIAA 1995-2358, 31st AIAA/ASME/SAE/ASEE Joint Propulsion Conference and Exhibit, San Diego, CA., 1995.

21. Choi, C.J., S.Y. Lee, and S.H. Song, *Disintegration of Annular Liquid Sheet with Core Air Flow − Mode Classification.* 1997. **24**(1-3): p. 399-406.

22. Kendall, J.M., *Experiments on annular liquid jet instability and on the formation of liquid shells.* Physics of Fluids, 1986. **29**(7): p. 2086-2094.

23. Park, J., et al., *Experimental investigation on cellular breakup of a planar liquid sheet from an air-blast nozzle.* Physics of Fluids, 2004. **16**(3): p. 625-632.

초 록

액체 분무에서 액적으로 이어지는 분무 분열은 산업 전반에 걸쳐서 이용되나 아직까지 분무 분열의 정확한 매커니즘이 완전히 밝혀지지 않았다. 산화제와 연료를 동축으로 분사하는 시스템은 액막의 분열을 가속화시킬 수 있으므로 동축 유동의 특성에 대한 연구가 오랫동안 이루어져 왔다.

분무 분열의 기본 매커니즘은 평면과 축대칭 유동에서 많이 연구되어 왔다. 넓은 종횡비의 평면 유동의 경우에는 표면 장력에 의한 가장자리 효과를 무시할 수 있으며 비교적 관찰하기 용이하므로 축대칭 유동에 비해 많이 연구되어왔다. 축대칭 유동의 경우 평면 유동과 크게 다르지 않으나 유동면 사이가 가깝기 때문에 표면장력에 의한 효과를 무시할 수 없다. 본 연구는 기체 중심 액체 환상형 액막에서의 분무 불안정 특성을 연구하였다. 분무 불안정에 의해 발생하는 액체 체적 불안정은 연소불안정으로 이어질 수 있다고 알려져 있다. 기체 중심 액체 환상형 분무에서의 불안정 특성을 관찰하기 위해 두 가지 실험이 수행되었다. 불안정 모드를 분류하고 불안정의 파장 길이를 측정하기 위해 간접 촬영기법이 사용되었다. 또한 분무 불안정의 주파수를 측정하기 위해 레이저를 이용하여 계측하였다.

본 연구에서는 먼저, 본 연구의 배경과 실험장치 및 실험 방법을 소개하였다.

두 번째로, 본 연구에서 관찰한 불안정 모드를 실험 조건에 따라

분류하고 각 불안정 모드에서 나타나는 불안정 특성을 분석하였다. 기체와 액체의 운동량비가 증가할수록 불안정 파장길이는 감소하고 주파수는 증가하였다. 본 연구에서 사용된 기하학적 변화로 선택된 리세스가 증가함에 따라서는 불안정 파장길이가 증가하고 주파수는 감소하였다.

본 연구의 결과를 통해 기체와 액체의 운동량비 뿐만 아니라 리세스비를 이용한 기하학적 형상의 변화 역시 분무 불안정에 영향을 줄 수 있음을 알 수 있다.

주요어: 기체 중심 액체 환상형 분사기, 간접 촬영 기법, 리세스비, 운동량비, 분무 불안정

학 번: 2010-23232